From Micro to Nano: Analysis of Surface-Enhanced Resonance Raman Spectroscopy Active Sites via Multiscale Correlations

ARTICLE *in* ANALYTICAL CHEMISTRY · FEBRUARY 2006

Impact Factor: 5.64 · DOI: 10.1021/ac051158a · Source: PubMed

6 AUTHORS, INCLUDING:

Imran Khan
Hazara University
6 PUBLICATIONS **230** CITATIONS
SEE PROFILE

Duncan Graham
University of Strathclyde
204 PUBLICATIONS **5,103** CITATIONS
SEE PROFILE

Ewen Smith
University of Strathclyde
345 PUBLICATIONS **8,257** CITATIONS
SEE PROFILE

From Micro to Nano: Analysis of Surface-Enhanced Resonance Raman Spectroscopy Active Sites via Multiscale Correlations

Imran Khan,*,† Dale Cunningham,‡ Rachael E. Littleford,‡ Duncan Graham,‡ W. Ewen Smith,‡ and David W. McComb†

Department of Materials, Imperial College London, London SW7 2AZ, UK, and Department of Pure and Applied Chemistry, University of Strathclyde, Glasgow G1 1XL, UK

Effective correlation of data from a number of analytical techniques over length scales spanning several orders of magnitude is required to more fully investigate the active sites on silver nanoparticles that are responsible for surface-enhanced resonance Raman scattering (SERRS). In this paper, a method is presented that uses fluorescent beads as optical markers to allow direct correlation between a SERRS/fluorescence map and a transmission electron microscope (TEM) collage of the same area. Factors influencing the accuracy of the technique include the flatness of the substrate, the size of the fluorescent beads, and the strength of the signal from the fluorescent beads. When the effect of each of these factors on the technique is addressed, a simple and accurate correlation between the optical spectroscopy and the electron microscopy is achieved. A statistically significant number of particles can then be easily and reliably located and characterized at both optical limits, by SERRS, and with subnanometer resolution in the high-resolution TEM. Examples of HRTEM images and the locations of these particles within the SERRS map/TEM collage are presented. Our findings reveal that the relative SERRS activity of single particles is very low compared to dimers and larger aggregates of particles. The relative activity of dimers is estimated to be 12.4 times greater than single particles, and as the number of particles in the aggregate increase, the relative SERRS activity also increases. The relative SERRS activities of single particles/dimers/trimers/aggregates of 4−9 particles/aggregates of 10−20 are estimated to be 1/12.4/15.6/23.2/43.

Nanoparticles exhibit unique optical and electronic properties and are of current interest for both fundamental studies and for potential application in nanoscale devices.[1−4] These properties may be tuned by controlling the nanoparticle shape, size, and state of aggregation.[1,2,5] Correlation of measurements from a number of techniques, with different resolutions and spanning many length scales from micro to subnanometer, are required to study nanoparticles more completely and to exploit the full power of today's technologies. In this paper, we describe a method that is uniquely capable of correlation of multiple analytical signals on multiple length scales to investigate the active sites for surface-enhanced resonance Raman spectroscopy (SERRS) from silver nanoparticles.

SERRS is a powerful analytical technique that is capable of single molecule detection and characterization.[6,7] These attributes represent the ultimate sensitivity and selectivity in nanoscale and ultratrace analysis, and there is great potential in the use of SERRS for analysis in many fields, including bioanalysis,[8−10] nanostructured materials,[11,12] and the detection of drugs[13] and chemical warfare agents.[14−16] Essential to the workings of SERRS is the adsorption of the analyte molecule to a roughened metal surface, usually silver or gold. Excitation of the molecule−metal complex with a laser of coincident or near-coincident wavelength to either or both the molecular chromophore or the surface plasmon resonance of the substrate will then afford a significant enhancement of the Raman scattering of the analyte molecule.

Raman enhancements of up to 10^6 are typically measured from analytes adsorbed to aggregated silver colloid systems.[17] In a few recent cases, enhancements of 10^8, from lithographically fabricated

† Imperial College London.

‡ University of Strathclyde.

(1) Kelly, K. L.; Coronado, E.; Zhao, L. L.; Schatz. G. C. *J. Phys. Chem. B* **2003**, *107*, 668.
(2) Hao, E.; Schatz, C. C. *J. Chem. Phys.* **2004**, *120*, 357.
(3) Storhoff, J. J.; Elghanian, R.; Micuc, R. C.; Mirkin, C. A.; Letsinger, R. L. *J. Am. Chem. Soc.* **1998**, *120*, 1959.
(4) Yonzon, C. R.; Jeoung, E.; Zou, S.; Schatz, G. C.; Mrksich, M.; Van Duyne, R. P. *J. Am. Chem. Soc.* **2004**, *126*, 12669.
(5) Jensen, T. R.; Malinsky, M. D.; Haynes, C. L.; Van Duyne, R. P. *J. Phys. Chem. B* **2000**, *104*, 10549.
(6) Emory, S. R.; Nie, S. *Science* **1997**, *275*, 1102.
(7) Kniepp, K.; Wang, Y.; Kneipp, H.; Perelman, L. T.; Itzkan, I.; Dasari, R. R.; Feld, M. *Phys. Rev. Lett.* **1997**, *78*, 1667.
(8) Docherty, F. T.; Monaghan, P. B.; Keir, R.; Graham, D.; Smith, W. E.; Cooper, J. M. *Chem. Commun.* **2004**, *1*, 118.
(9) Cao, Y. W. C.; Jin, R. C.; Mirkin, C. A. *Science* **2002**, *297*, 1536.
(10) Faulds, K.; Barbagallo, R. P.; Keer, J. T.; Smith, W. E.; Graham, D. *Analyst* **2004**, *129*, 567
(11) Mirkin, C. A.; Letsinger, R. L.; Micuc, R. C.; Storhoff, J. J. *J. Am. Chem. Soc.* **1996**, *382*, 607.
(12) Haynes, C. L.; Van Duyne, R. P. *J. Phys. Chem. B* **2003**, *107*, 7426.
(13) Littleford, R. E.; Matousek, P.; Towrie, M.; Parker, A. W.; Dent, G.; Lacey, R. J.; Smith, W. E. *Analyst* **2004**, *129*, 505.
(14) McHugh, C. J.; Keir, R.; Graham, D.; Smith, W. E. *Chem. Commun.* **2002**, *6*, 580.
(15) McHugh, C. J.; Keir, R.; Graham, D.; Smith, W. E. *Chem. Commun.* **2002**, *21*, 2514.
(16) Zang, X. Y.; Young, M. A.; Lyandres, O.; Van Duyne, R. P. *J. Am. Chem. Soc.* **2005**, *127*, 4484.
(17) Moscovits, M. *Rev. Mod. Phys.* **1985**, *57*, 783.

silver torroids,[18] and 10^9, from an evaporated silver−analyte−nanoparticle sandwich complex,[19] have been reported. In these reports, the SERRS signals are collected from a large number of nanostructures present on the substrate, and the enhancements measured are averaged over all of these nanostructures. When individual nanostructures have been analyzed and only one SERRS active site or particle or active species is considered, Raman enhancements of up to 10^{15} are reported. This level of sensitivity enables detection of a single molecule.[6,7,20] Both a dominant electromagnetic and a weaker chemical enhancement mechanism are considered to operate in SERRS systems. Although the general details of these mechanisms are broadly accepted,[17,21] the processes occurring at SERRS active sites, where enormous enhancements of the Raman signal occur, are poorly understood.

The analysis of SERRS from analyte molecules adsorbed to silver particles has been one of the most informative ways of studying the SERRS mechanism, and the different systems studied include isolated single particles,[6,22,23] dimers,[20,22−24] and clusters,[22,23,25−27] as well as ensemble-averaged measurements from thousands of aggregated particles.[7,28] In addition to facilitating the practical and quantitative use of SERRS in ultrasensitive analysis, the intrinsic differences in SERRS activity, in origin possibly microstructural, chemical/electronic, or both, between silver nanoparticles is of great fundamental interest. Experimental methods and theoretical models need to be developed to measure, predict, and understand the processes by which some but not all silver nanoparticles or clusters of particles are SERRS-active. In previous studies, we have developed an effective method for the analysis of a statistically significant number of immobilized nanoparticles by both SERRS and TEM.[22,23] This method involves the correlation of a SERRS map, recorded using an optical microscope, with a collage of transmission electron microscope (TEM) images of the same area of the substrate. Correlation of the optical measurements with the TEM images required the starting and ending points of the map to be measured and these measurements transferred to the TEM images. This method is limited by the accuracy with which it is possible to measure the coordinates of the starting and ending points using the optical microscope.

In this paper, we describe a significant improvement to this method through the use of fluorescent beads as optical markers. Each fluorescent bead is visible in both the optical and TEM images and also exhibits a fluorescence spectrum that is easily identifiable in the SERRS map. When three or more beads are present in the analyzed area, triangulation is possible, and correlation of the SERRS map with the optical and TEM images is achievable by overlaying each fluorescence signal with the image of the corresponding bead. In this way, the SERRS map can be set to the correct size and can be accurately superimposed on the TEM collage. Using this approach, the coordinates of the analyzed area are not required, and a fast and simple correlation of the data is achieved. SERRS-active and -inactive particles may then be unambiguously identified and characterized using the high-resolution analytical TEM. A further advantage of this technique is that a statistically significant number of individual particles and aggregates of particles are analyzed efficiently, and the percentage that are active can be determined. In this way, the relative SERRS intensities of single particles, dimers, trimers, and larger aggregates can be measured.

EXPERIMENTAL SECTION

Raman spectra were obtained using a Renishaw Raman InVia system in confocal setup equipped with a Spectra Physics 514.5 Ar^+ laser and Renishaw *XYZ* mapping stage. With a ×100 objective, the lateral resolution of the Raman system was measured to be ~1 μm. For all experiments, the laser power at the sample was measured to be 15 μW, and an accumulation time of 1 s was used. Under these conditions, no photodegradation of the particle−dye complex occurs.[22] The Raman equipment was set up on a vibration-free table. Without the vibration-free table, the system was not suitable for the collection of Raman signals from the TEM grid because any disturbance in the room caused the stage and objective to shift such that the substrate was out of focus.

Electron microscopy was performed using a JEOL 2010 TEM, operating at 200 kV and fitted with a LaB_6 filament. A Gatan Multiscan digital camera was used for image capture. The images were processed using Gatan Digital Micrograph software.

Silver colloid and the analyte dye, 3,5-dimethoxy-4-(5′-azobenzotriazoyl) phenylamine, ABT-DMOPA, were prepared as described previously.[22] Fluorescent beads were obtained from P.A.R.I.S. Beads, Paris, France, and Bangs Labs, Inc., Indianapolis, IN. The beads contained the fluorescent dye Rhodamine 6G chemically bound to the bead surface. Silver colloid was immobilized on labeled SiO_x TEM grids (SPI, West Chester, PA) in a manner similar to that described previously.[22] However, for all experiments detailed here, the grids were not coated with Formvar and were not silanized. In brief, each grid was rinsed in methanol and allowed to dry, and 1 drop of a dilute colloid was placed on one side of the grid and allowed to evaporate completely. The grid was rinsed in water and then methanol before 1 drop of analyte dye (ABT-DMOPA, 1×10^6 M) was applied to the same side of the grid. After 5 min, the excess dye was washed from the grid by immersion in methanol. A suspension of fluorescent beads in methanol was diluted to a suitable concentration, then 1 drop was applied to the same side of the grid. After 5 min, the grid was rinsed in methanol then allowed to dry before analysis.

RESULTS AND DISCUSSION

In these experiments, beads measuring ~900 nm or 2 μm in diameter with relatively high or relatively low fluorescence intensity were used. The fluorescence map is constructed by plotting the intensity of the spectral background at 1800 cm^{-1} against the spatial coordinates. The SERRS map of the same area

(18) Liu, F. M.; Green, M. *J. Mater. Chem.* **2004**, *14*, 1526.
(19) Orendorff, C. J.; Gole, A.; Sau, T. K.; Murphy, C. J. *Anal. Chem.* **2005**, *77*, 3261.
(20) Xu, H.; Bjerneld, E. J.; Kall, M.; Borjesson, L. *Phys. Rev. Lett.* **1999**, *83*, 4357.
(21) Campion, A.; Kambhampati, P. *Chem. Soc. Rev.* **1998**, *27*, 241.
(22) Khan, I.; Polwart, E.; McComb, D. W.; W. E.; Smith, *Analyst* **2004**, *129*, 950.
(23) Khan, I.; Cunningham, D.; Graham, D.; McComb, D. W.; Smith, W. E. *J. Phys. Chem. B* **2005**, *109*, 3454.
(24) Xu, H.; Aizpurua, J.; Kall, M.; Apell, P. *Phys. Rev. E*, **2000**, *62*, 4318.
(25) Markel, V. A.; Shalaev, V. M.; Zhang, P.; Huynh, W.; Tay, L.; Haslett, T. L.; Moscovits, M. *Phys Rev. B* **1999**, *59*, 10903.
(26) Michaels, A. M.; Nirmal, M.; Brus, L. E. *J. Am. Chem. Soc.* **1999**, *121*, 9932.
(27) Michaels, A. M.; Jiang, J.; Brus, L. E. *J. Phys. Chem. B* **2000**, *104*, 11965.
(28) Hildebrandt, P.; Stockburger, M. *J. Phys. Chem.* **1984**, *88*, 5935.

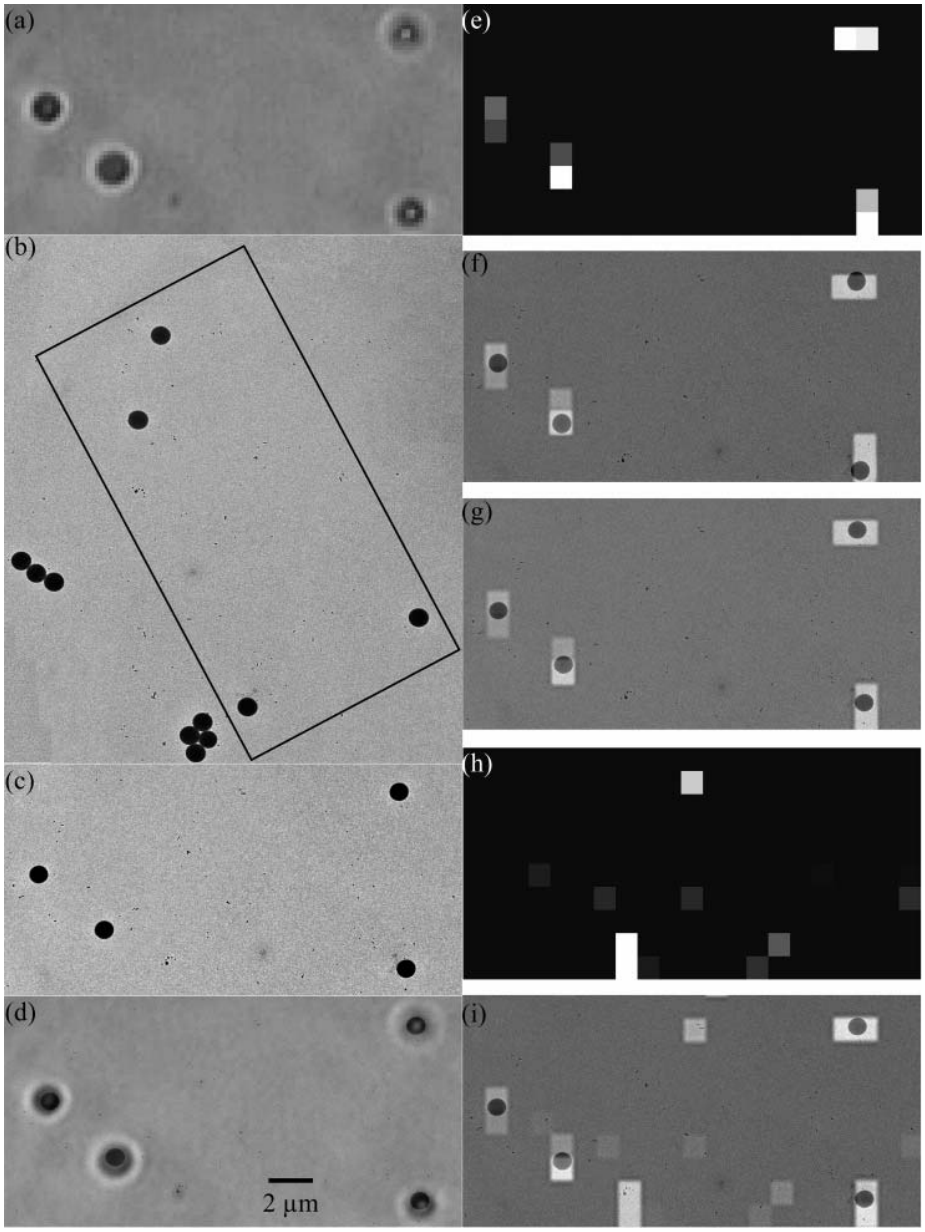

Figure 1. Use of fluorescent beads as optical markers for correlation of a SERRS map with a TEM collage. (a) Optical image showing the analyzed area containing four fluorescent beads. (b) Collage of TEM images at different orientation; the rectangle indicates the analyzed area. At this resolution, the silver nanoparticles are present as dark dots. (c) TEM collage orientated to match the optical image and SERRS/fluorescence maps. (d) Optical and TEM images superimposed. (e) Fluorescence map. (f) Fluorescence map superimposed on TEM collage; poor correlation. (g) Fluorescence map stretched and superimposed on TEM collage for good correlation. (h) SERRS map set to same dimensions as fluorescence map. (i) SERRS map superimposed on fluorescence map and TEM collage. All images are set to the same scale.

is constructed using the intensity of the strongest peak in the SERRS spectrum of the analyte dye.[22] It should be noted that the SERRS and fluorescence data are accumulated simultaneously, and one map contains both data sets.

Each step in the process of correlating the SERRS/fluorescence intensity map with the low magnification TEM collage of the same area is presented in Figure 1. The optical image obtained from the Raman microscope shows the area analyzed by SERRS mapping (Figure 1a). This area is a region within a specific grid square of a lettered TEM grid that may be located in both the optical and electron microscopes by its position in relation to a letter. The image shows four fluorescent beads present in the area of interest, each measuring ~900 nm in diameter, although the silver nanoparticles on the grid are not observed with the optical microscope. The TEM collage of the same area is indicated by a rectangle in Figure 1b. Here, both the beads and the silver particles are visible, although the orientation of the image is different from the optical image. In Figure 1c, the TEM collage is rotated to the same orientation as the optical image, and in 1d, the optical image is overlaid on the TEM image. This is achieved by scaling the optical image to the same dimensions as the TEM collage. In all experiments, no change in the aspect ratio of the optical image is required to achieve a perfect fit with the TEM collage. The scaling factor applied to the optical image can now

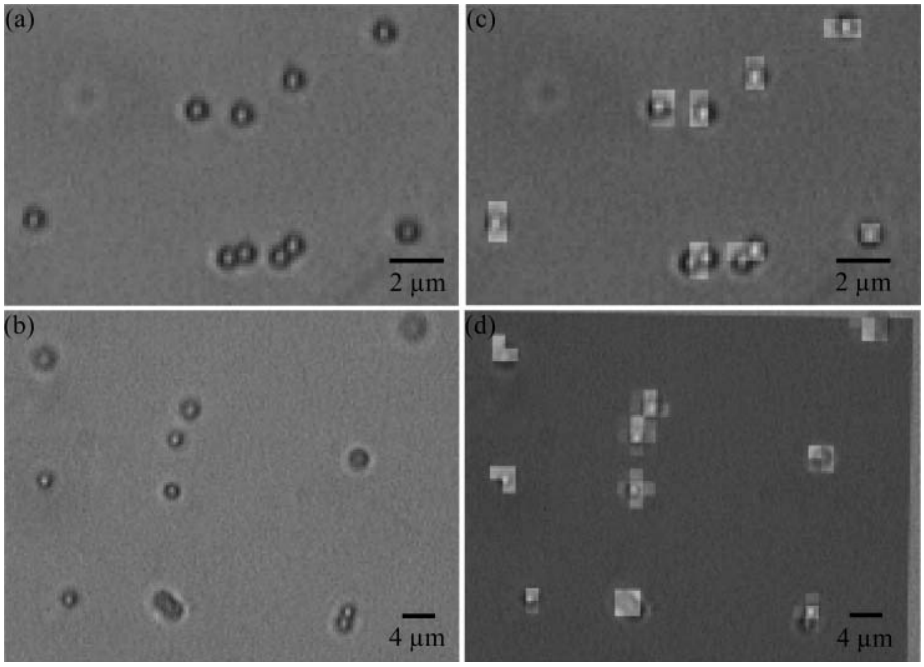

Figure 2. (a,b) Optical images and (c, d) optical images with fluorescence maps superimposed of mapped areas containing fluorescent beads.

be applied to the fluorescence intensity map (Figure 1e). When the fluorescence map is overlaid on the TEM collage, a slight mismatch between the bead image and the fluorescence intensity is apparent (Figure 1f). To correct this mismatch and achieve a good correlation, it is necessary to distort the fluorescence map by changing the aspect ratio. In this case, the height of the map is decreased by 4% while the width of the map is unchanged. When the altered fluorescence map is superimposed on the TEM collage (Figure 1g), improved correlation is achieved. The SERRS map may then be scaled to the same dimensions as the altered fluorescence map (Figure 1h) and superimposed onto the TEM collage to allow each of the SERRS signals to be assigned to a silver particle or number of particles (Figure 1i). Clearly, this distortion of the fluorescence/SERRS map to achieve a best fit is subjective and undesirable. A high precision correlation of the data is required to give a confident assignment of SERRS activity or inactivity to specific particles.

From a number of experiments, a poor correlation between the fluorescence/SERRS map and the TEM collage was observed. This mismatch was not systematic, suggesting that a misalignment of the Raman spectrometer was not the cause. Instead, the mismatch and the correction required for a good correlation were found to be random between experiments and could be small or significant. The size of bead or fluorescent intensity detected from the bead used did not affect this mismatch. In Figure 2, a good correlation between the fluorescence map and the TEM collage is achieved by scaling the size of the map without changing the aspect ratio. In this case, each of the six single beads and the two dimers of beads overlay perfectly with the associated fluorescence intensity. On careful inspection, it can be seen that each of the beads in Figure 2 is in sharp focus. Contrast this with the optical image in Figure 1 where, although two of the beads are in focus, two of the beads and, therefore, part of the analyzed area were out of focus. Analysis of the many maps run revealed that when not all of the analyzed area is in sharp focus with the $\times 100$ objective, a mismatch occurs between the bead images and the fluorescence intensity. When the entire area to be mapped is in sharp focus, there is a strong correlation between the beads and the fluorescence intensity. This conclusion was tested further in an experiment in which a grid was analyzed that was buckled very slightly such that the area to be mapped was not flat. Buckling of the grid may have occurred during grid preparation. The same area from the grid was analyzed twice, once with the grid simply placed onto a glass slide and second with the grid held flat, using thin glass slides positioned round the edge of the grid. In the first case, a mismatch between the data was observed, as expected. In the second case, however, the data correlated perfectly. In this case, the slight buckling of the grid is corrected to leave the mapped area flat and in focus. A special sample holder was built to fit onto the Raman microscope stage and to hold the TEM grid flat. The TEM grids used contain undulations in the thin SiO_x film that can also produce "bumpy" areas of the grid. If the area to be analyzed contains these undulations, flattening of the grid itself does not flatten out the bumps in the film. Therefore, for a good correlation of the data, it is essential for the area analyzed to be flat, as viewed through the optical microscope with the $\times 100$ objective. The optical image from the Raman microscope is transferred vertically to the eyepiece and the digital camera; however, the scattered light is reflected at right angles before entering the spectrometer and the CCD detector. If the substrate is not flat, signals from different points on the grid will reach the CCD at different angles, and the pixels of the map will be nonuniform. Consequently, there may be a mismatch between data displayed in a pixel and the position on the grid from which the data was collected. On a flat grid surface, these mismatch effects do not occur, and there is a good correlation between data detected by the CCD and the position on the grid from which the data was collected. The fluorescence map can therefore be correlated precisely with the TEM collage without alteration to the aspect ratio. The confident assignment of SERRS activity to

specific particles can now be made. The effect of the grid morphology has been considered before, although only with regard to the SERRS collection efficiency from the immobilized silver particles.[22]

The effect of the size of the beads on the fluorescence map is demonstrated in Figure 2. In Figure 2a,c, 900-nm-diameter beads are used, and fluorescence intensity is detected in only 1 or 2 pixels of the map. In Figure 2b,d, 2-μm-diameter beads are used, and each bead is associated with 3−5 fluorescent pixels. In terms of accuracy, there is little practical difference between the use of either size of bead, and in each case, a good or bad correlation is easily observed. The use of 900-nm beads is preferable, since they occupy fewer pixels on the map and, hence, do not obscure the SERRS intensity from particles located close to a bead. Beads significantly smaller than the pixel size (~500-nm diameter) are more likely to be detected in one pixel only; however, the positioning of a bead within a pixel cannot be defined accurately, and an improvement in accuracy may not result. With regard to the number of beads used for correlation, the results suggest that the use of three beads is sufficient and that increased numbers of beads do not improve the correlation significantly.

The use of beads that exhibit more intense fluorescence (~100 times stronger than the beads used in Figures 1 and 2) has also been investigated. Figure 3a and b shows the TEM collage and the fluorescence map for 900-nm-diameter beads that are strongly fluorescent. Here, fluorescence from one bead is detected in up to 12 pixels. This result can be explained by considering the resolution of the Raman system. The lateral resolution of the Raman system is estimated by measuring the intensity detected from a silicon wafer as the objective is moved away from the source. An intensity profile is drawn, and the resolution of the system is taken to be the distance at which the intensity drops to one-half the original. Using this method, the lateral resolution of the Raman system is measured to be ~1 μm. However, there is a long tail on the intensity profile such that intense signals are detected at distances from the source that are greater than the resolution. In this case, each bead signal is of sufficient intensity to be detected 1 or 2 μm from the edge of the bead in all directions.

To use these beads as optical markers, it is necessary to better define the fluorescence intensity with regard to the position of the bead. Therefore, each fluorescent pixel exhibiting less than one-half the maximum intensity detected from a particular bead is removed from the fluorescence intensity map. In essence, the fluorescence intensity detected from pixels located at a distance from the edge of a bead that is beyond the resolution of the system are omitted. Figure 3c shows the fluorescence map obtained after this operation. For each bead, there are now only two pixels exhibiting relatively strong intensity, and a good correlation through triangulation of the three sets of fluorescence signals with the three beads is possible. The SERRS map, scaled to the same dimensions as the bead map, is shown in Figure 3d; the correlation between the TEM collage, the fluorescence map, and the SERRS map is presented in Figure 3e. Each of the light-colored pixels in the SERRS map represents a pixel from which a SERRS spectrum has been detected. We define each of these pixels as a "SERRS-active pixel". The dark pixels represent areas of the substrate from which no SERRS spectra are detected. The SERRS-active and -inactive particles can now be clearly identified within the SERRS-active and -inactive pixels. It should be noted that for particles in close proximity to the fluorescent beads, the SERRS signals were often obscured completely by the strong fluorescent emission. It is therefore not possible to measure the SERRS activity of these particles, and they were omitted from the study. A major advantage of this technique is that a statistically significant number of active and inactive particles and aggregates are identified, and it is possible to determine the relative SERRS activities of each of these species.

From our previous work,[23] we have measured the SERRS intensities from a large number of individual particles and aggregates of particles. However, to compile these results, it was necessary to discard a number of data sets when the correlation was not clear and an assignment of SERRS activity could not be made unequivocally. In the study presented here, with the use of fluorescent beads to allow confident correlation, all the results could be used. In Table 1, the percentage of active single particles, dimers, trimers, and larger clusters are presented against the total number analyzed. The data are compiled from a total of four separate maps, and two different batches of colloid were analyzed. As was discussed in our previous work, [23] it is sometimes the case that more than one particle or aggregate is present in an active pixel, and the SERRS intensity may be detected from one or all of these species present. In Table 1, the "maximum" number of active particles includes all particles that are present in active pixels. Obviously, this process will overestimate the number of active species. The most accurate analysis of the data is achieved by only considering cases for which individual species are present in an active pixel. In Table 1, the "minimum" value includes only those particles that are present individually in an active pixel. To illustrate the interpretation of this table, consider the dimer species. In all four maps, 50 dimers were analyzed. Of these, 14 dimers were present in SERRS-active pixels where no other species was present, and 12 dimers were present in SERRS-active pixels where another species was also present. This leads to the maximum and minimum values entered in columns 3 and 4.

In Table 1, we observe that, in general, the percentage of a species that is active increases with the number of aggregated particles present, and these results are in keeping with our previous findings.[23] The most striking observations from Table 1 are the high SERRS activities of aggregates relative to single particles and how few single particles are active. Only 2.3% of spatially isolated, individual, single particles are active, as compared to 28% in the case of dimers. This significant increase in SERRS efficiency of dimers over single particles might be due to the creation of interparticle sites of high electromagnetic field strength upon the aggregation of particles. From Table 1, as the number of aggregated particles increases from 2 to 9, a more gradual increase in the percentage of active species is observed. These results suggest that the presence of more interparticle sites does not greatly improve the SERRS enhancement, and there is only a slight increase in SERRS activity per particle. Each of the six aggregates that were analyzed containing 10 particles or more are active, although more data would be required before it would be possible to observe if all aggregates of this size are active. In our previous study, the relative activity of dimers was measured to be only twice that of single particles.[23] The colloid used here is

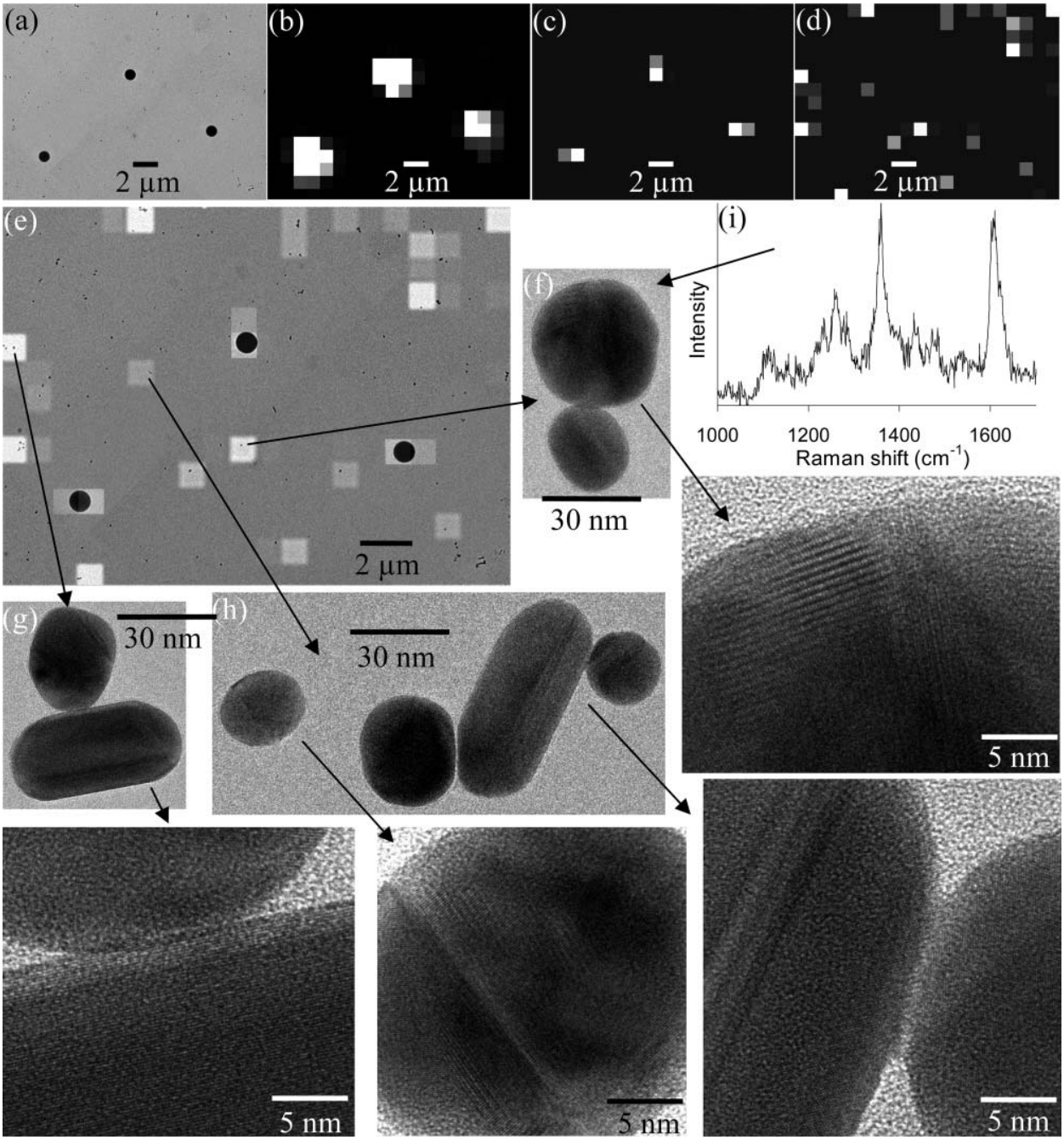

Figure 3. Identification and characterization of SERRS-active and -inactive silver particles. (a) Collage of TEM images. (b) Fluorescence intensity map. (c) Fluorescence intensity map showing significant fluorescence intensity only. (d) SERRS intensity map of the same area of the substrate. (e) Fluorescence and SERRS maps overlaid on the TEM collage to allow identification and HRTEM imaging of two SERRS active dimers (f,g) and one SERRS-active cluster (h). (i) SERRS spectrum recorded from dimer (f).

prepared following the same procedure and has a particle size distribution similar to that used previously. However, the previous study revealed that the SERRS activities of colloids prepared by the same procedure could vary significantly. We therefore conclude that the relative SERRS activity of single particles varies from one batch of colloid to another.

On average, the SERRS intensities detected from a particular species increase with the number of aggregated particles, although for all species, the intensities range from zero to very high. These results indicate that in addition to the number of particles present, a number of other factors contribute to the measured SERRS activity. When estimating the relative SERRS activities of single particles and aggregates, it is therefore more informative to use the percentage of species that are active and not the SERRS intensities measured. The ratio of the percentage of active single particles/dimers/trimers/aggregates of 4−9 particles/aggregates of 10−20 is estimated to be 1/12.4/15.6/23.2/43, and these ratios serve as a good estimate of the relative SERRS activities. Each of these active and inactive particles and aggregates can be studied in the HRTEM. For example, HRTEM images of two SERRS-active dimers and an active cluster are shown in Figure 3; the positions of these particles within the map are indicated. The SERRS

Table 1. Number of Particles or Aggregates of Particles Analyzed and Detected from Four Maps of Two Different Colloids

species	no. analyzed	no. active maximum, minimum[a]	SERRS intensity range (av)	% active maximum, minimum
single particles	172	19, 4	90−275 (181)	11, 2.3
dimers	50	26, 14	40−1135 (190)	52, 28
trimers	11	6, 4	68−265 (125)	54.6, 36.4
small aggregates (4−9 particles)	13	8, 7	40−1000 (251)	62, 54
large aggregates (10−20 particles)	6	6, 6	220−1030 (460)	100, 100
total	252	65, 35	40−1135 (204)	25.8, 13.9

[a] The minimum number of active species indicates the number of active species sufficiently spaced such that each species was analyzed individually. The maximum number of active species indicates all active species present in active pixels, even when two or more species are present. For example, consider the dimer species. In all four maps, 47 dimers were analyzed. Of these, 12 dimers were present in SERRRS-active pixels where no other species was present, and 9 dimers were present in SERRS-active pixels where another species was also present. The values quoted for the intensity ranges are taken from isolated species only.

spectrum collected from one of the dimers is also shown. HRTEM imaging, together with electron diffraction analysis, allows the particle microstructure to be determined. Within the HRTEM images (Figure 3), the silver lattice planes are visible, and a number of features are present that may or may not be associated with SERRS enhancement. These features include the presence of crystal defects within particles, such as twin boundaries; stacking faults and dislocations; and the dimensions of the spacings between aggregated particles or whether particles are touching or overlapping. A detailed diffraction analysis is required to fully characterize each of the crystal defects. In other reports, we have studied HRTEM images of SERRS-active and -inactive particles, but to date, no clear correlation between the presence of particle defects or narrow interparticle sites with high SERRS activity have been observed.[23,29]

Since this method allows positive identification of specific particles within different instruments, techniques such as energy dispersive spectroscopy and electron energy loss spectroscopy can be used to obtain information on the microstructure, composition, and the electronic and chemical properties of SERRS-active and -inactive particles. Investigations in this area are ongoing.

CONCLUSIONS

The use of fluorescent beads as optical markers has been developed to allow a fast and reliable method for the correlation of a SERRS/fluorescence map with a TEM collage of the same area. Fluorescent beads of different sizes and fluorescence intensity have been studied and compared for their suitability for use as optical markers. The accuracy of the correlations based on their use has also been assessed. Of key importance to obtaining a good correlation between SERRS/fluorescence and TEM measurements is to have a flat substrate. If a TEM grid is slightly buckled or if the SiO_x film of the analyzed area contains undulations, then a poor correlation is obtained, and the SERRS/fluorescence map must be distorted to fit. It is quite common for the grid to buckle slightly upon preparation, and if the grid is silanized, distortions to the grid are usually more pronounced. Use of this method has allowed significant numbers of SERRS active and inactive particles to be unambiguously identified and characterized. In this study, it has been found that the percentage of dimers that are SERRS-active is significantly greater than the percentage of active single particles. As the number of particles present in the aggregate increases, the relative SERRS activity also increases, and the relative SERRS activities of single particles/dimers/trimers/aggregates of 4−9 particles/aggregates of 10−20 are estimated to be 1/12.4/15.6/23.2/43.

In future studies, a significant number of particles must be studied in the HRTEM to aid understanding of the relationship between SERRS activity and particle microstructure, particle interactions and the electronic and chemical properties of particles and aggregates of particles. Multiscale correlations between measurements performed in a number of different instruments may also be of great potential use to the study of other systems.

(29) Khan, I.; Cunningham, D.; Graham, D.; McComb, D. W.; Smith, W. E. Accepted by *Faraday Discussions FD132*. DOI: 10.1039/b506644a.

ACKNOWLEDGMENT

We thank the EPSRC for funding of this research.

Received for review June 29, 2005. Accepted October 19, 2005.

AC051158A